JACS
JOURNAL OF THE AMERICAN CHEMICAL SOCIETY

COMMUNICATION

pubs.acs.org/JACS

Paramagnetic Bridging Hydrides of Relevance to Catalytic Hydrogen Evolution at Metallosulfur Centers

Aušra Jablonskytė,[†] Joseph A. Wright,[†] Shirley A. Fairhurst,[‡] Jamie N. T. Peck,[†] Saad K. Ibrahim,[†] Vasily S. Oganesyan,[†] and Christopher J. Pickett*[,†]

[†]Energy Materials Laboratory, School of Chemistry, University of East Anglia, Norwich Research Park, Norwich NR4 7TJ, U.K.

[‡]John Innes Centre, Norwich Research Park, Norwich NR4 7UH, U.K.

Supporting Information

ABSTRACT: Paramagnetic hydrides are likely intermediates in hydrogen-evolving enzymic and molecular systems. Herein we report the first spectroscopic characterization of well-defined paramagnetic bridging hydrides. Time-resolved FTIR spectroelectrochemical experiments on a sub-second time scale revealed that single-electron transfer to the μ-hydride di-iron dithiolate complex **1** generates a 37-electron valence-delocalized species with no gross structural reorganization of the coordination sphere. DFT calculations support and ^{1}H and ^{2}H EPR measurements confirmed the formation an $S = {}^{1}/_{2}$ paramagnetic complex ($g = 2.0066$) in which the unpaired spin density is essentially symmetrically distributed over the two iron atoms with strong hyperfine coupling to the bridging hydride ($A_{iso} = -75.8$ MHz).

Understanding the chemistry that takes place at the active site of [FeFe]-hydrogenase, the H-cluster, is of both high intrinsic interest and potential technological impact in the context of hydrogen generation and utilization.[1,2] One aspect of this chemistry is the role of bridging and/or terminal iron hydrides as transient intermediates during the turnover of the enzyme. Much work has been done on the isolation and spectroscopy of closed-shell synthetic bridging and terminal hydrides, which can be formed by protonation of electron-rich Fe(I)−Fe(I) dithiolate analogues of the H-cluster subsite. Many stable Fe(II)−Fe(II)-bridging hydrides formed in this way have been crystallographically and spectroscopically characterized,[3−5] while the structure of a terminal hydride di-iron dithiolate that was synthesized indirectly has also been described.[6] Low-temperature NMR studies have established the formation of terminal hydrides as kinetic intermediates on the pathway to the thermodynamically more stable bridging species.[7−9] Mechanistic studies detailing the formation of the hydride-bridged diiron dithiolates $[HFe_2(pdt)(CO)_4(PMe_3)_2]^+$ (**1**) (pdt =1,3-propanedithiolate)[3] and $[HFe_2(edt)(CO)_4(PMe_3)_2]^+$ (**2**) (edt =1,2-ethanedithiolate)[10] (Figure 1) by FTIR stopped-flow protonation experiments have been reported.[11]

Mixed-valence Fe(I)−Fe(II) hydrides have been postulated as intermediates in the turnover of the enzyme and also in electrocatalysis of proton reduction mediated by synthetic Fe(I)−Fe(I) subsite analogues.[12−15] Quantum mechanics/molecular mechanics (QM/MM) studies (which of course outpace empiricism) suggest that only protonated Fe(I)−Fe(II) systems are competent for dihydrogen evolution.[16] De Gioia has noted from density functional theory (DFT) calculations that dihydrogen formation may occur via mixed-valence Fe(I)−Fe(II) μ-hydride species.[17] It is with such as yet unisolated and spectroscopically uncharacterized Fe(I)−Fe(II) hydrides that we are now concerned.[18]

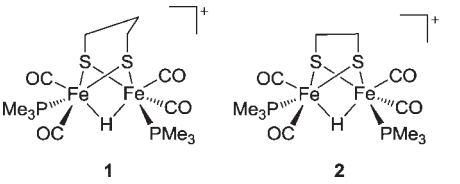

Figure 1. Protonated structural models for the subsite of [FeFe]-hydrogenase.[3,10]

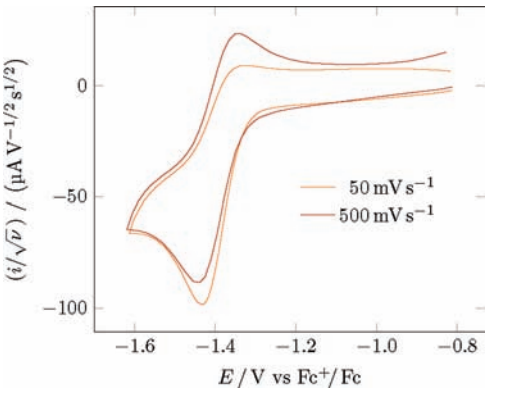

Figure 2. Normalized cyclic voltammograms of **1** (10 mM) recorded at a vitreous carbon working electrode in MeCN containing 0.1 M $[Bu_4N][BF_4]$ at 25 °C. The potential scale is set relative to the ferrocenium/ferrocene (Fc^+/Fc) couple.

The evidence that such mixed-valence hydrides exist rests solely with cyclic voltammetric experiments showing the generation of more or less unstable species by reduction of Fe(II)−Fe(II) hydride precursors.[19] This is illustrated by the (scan rate)$^{1/2}$-normalized voltammograms for the reduction of the bridging hydride complex **1** at 50 mV s^{-1} and 500 mV s^{-1},

Received: September 16, 2011
Published: October 28, 2011

which were recorded at 25 °C (Figure 2). The reduction process is partially reversible at the lower scan rate and approaches full reversibility at the higher scan rate, indicative of the neutral primary one-electron reduction product having a half-life of ca. 1 s under these conditions. The behavior of **2** under the same conditions is similar, but the primary product is less stable.

Since the model subsites are redox-active and also bear strong IR chromophores (CO), time-resolved spectroelectrochemistry (SEC) has the potential to reveal significant detail about molecular changes accompanying electron transfer.[20] To this end, we used an attenuated total reflectance thin-layer SEC device to record time-resolved data. This allowed us to obtain the first IR data for two mixed-valence Fe(I)−Fe(II) hydride-bridged species: well-defined IR spectra of the primary one-electron reduction products of the bridging hydrides **1** and **2** were measured.

SEC measurements were conducted under an atmosphere of dinitrogen in a 0.1 M $[Bu_4N][BF_4]$ solution in MeCN. The potential was stepped from ca. 1100 mV positive of $E_{1/2}$, at which **1** and **2** are inactive, to ca. 300 mV negative of $E_{1/2}$, at which they are reduced in the thin layer at a diffusion-controlled rate.

The parent compound **1** exhibits two peaks in the carbonyl region at 2031 and 1989 cm^{-1}. Upon reduction, these are rapidly replaced by two new bands at 1948 and 1900 cm^{-1} (Figure 3, top). The primary product has a half-life of ca. 1.6 s, as measured by the loss of the absorption at 1948 cm^{-1}. The ethanedithiolate analogue **2** exhibits a similar pattern of reactivity, with the starting-material signals at 2035 and 1994 cm^{-1} being replaced by maxima at 1951 and 1902 cm^{-1}. In this case, the intermediate is shorter lived and has a half-life of ca. 0.4 s,[21] fully concordant with the cyclic voltammetry data. The reversibility of the system was confirmed by a double potential step experiment: switching back to the initial potential 1 s after the reduction step regenerated the spectrum of the starting material (Figure S1 in the Supporting Information).

SEC of **1** in THF revealed that the same spectral changes occur upon generation of the primary product, with identical peak maxima (Figure 3, bottom). Although the higher resistivity of THF incurs a longer cell response time, the greater stability of the one-electron-reduced primary product, which has a lifetime of ca. 7 s, compensates for this. We therefore used this solvent when generating the radical for EPR spectroscopy.

In the primary reduction of **1** and **2**, the retention of the peak pattern of the starting material suggests that the first-formed intermediate has the same geometry as the parent compound, i.e., that there is no gross structural change following single-electron transfer. While the reduced intermediate is formally a mixed-valence Fe(I)−Fe(II) species, the IR data suggest that it is better described as a 37-electron valence-delocalized system containing two Fe atoms with an average oxidation state of 1.5.

DFT simulations of both **1** and **2** and their singly reduced forms were undertaken (for full details, see the Supporting Information). In both cases, the simulated IR spectra are in accord with the experimental observation that reduction leads to a shift in the positions of the peak maxima but not to the development of any additional signals. This is because the basal/basal transoid geometry of the parent hydride is retained upon single-electron reduction, as it is the most stable isomer.[22]

Compound **1** was reduced using the acenaphthylene monoanion radical ($E_{1/2}$ = −2.12 V vs Fc^+/Fc) in THF at 195 K and examined using EPR spectroscopy. Figure 4 (top) shows the well-defined isotropic solution $S = {}^1/_2$ spectrum obtained at 165 K. Analysis revealed that this EPR spectrum is characterized by a g factor of 2.0066 and strong hyperfine interactions with three nuclei:

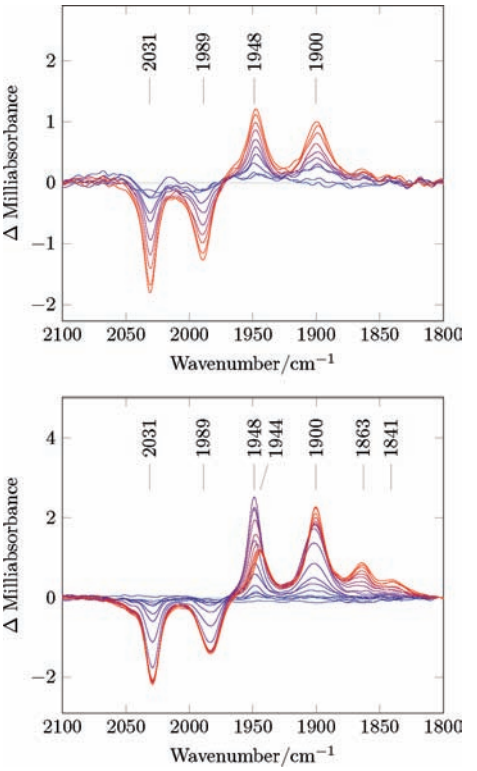

Figure 3. (top) Difference spectrum for the reduction of **1** in the time range 0.25 s (blue) to 1.79 s (red) relative to a scan at 0.08 s ($[\mathbf{1}]_0$ = 10 mM in MeCN containing 0.1 M $[Bu_4N][BF_4]$, 25 °C). (bottom) Difference spectrum for the reduction of **1** in the time range 1.0 s (blue) to 24.2 s (red) relative to a scan at 0.3 s ($[\mathbf{1}]_0$ = 10 mM in THF containing 0.2 M $[Bu_4N][BF_4]$, 25 °C).

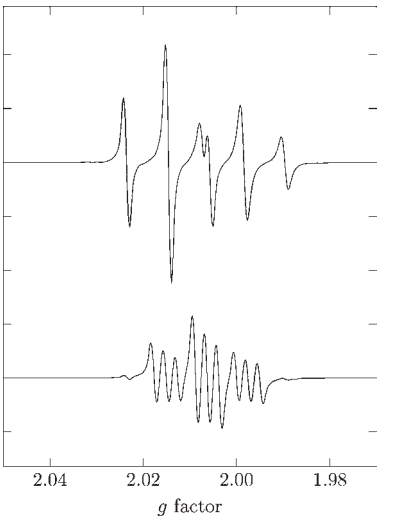

Figure 4. Continuous-wave X-band EPR spectra in THF: (top) reduced **1** at 165 K; (bottom) reduced *deutero*-**1** at 164 K. The line-width variation across the spectra, which is due to the sign of the coupling constants, is most pronounced in the spectrum of reduced *protio*-**1**.

two equivalent phosphorus atoms (A_{iso} = −41.7 MHz) and the bridging hydride (A_{iso} = −75.8 MHz).[23] The assignment of the latter was confirmed by the reduction of bridge-deuterated **1**. The spectrum of this species (Figure 4, bottom) shows the anticipated

dx.doi.org/10.1021/ja2087536 |J. Am. Chem. Soc. 2011, 133, 18606–18609

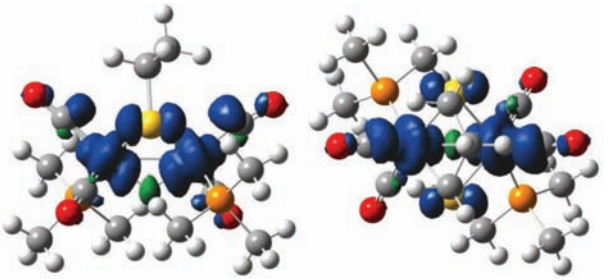

Figure 5. Isosurface of the spin density distribution of the singly reduced form of **1**: (left) side view; (right) top view. The spin density phases are indicated in blue and green. The spin density distribution of the singly reduced form of **2** is broadly similar.

1:1:1 splitting for coupling to the bridging deuteride, with the coupling constant reduced by the magnetogyric ratio γ_D/γ_H[24] ($A_{iso} = -11.6$ MHz); the phosphorus coupling is unchanged. This pattern of coupling is in accord with a symmetrical disposition of the radical character.

DFT simulations indicate that spin density is primarily localized on the iron atoms (Figure 5), with the iron centers in **1** bearing a total of 70% of the unpaired electron density.[25] Approximately 3% of the calculated spin density is located on the bridging hydride, while the two phosphorus atoms bear a total of 0.5%. In combination with the standard isotropic atomic hyperfine coupling values (1420 MHz for ^{1}H and 10 178 MHz for ^{31}P),[26] the experimental coupling constants can be used to find empirical spin density dispositions: 5% for the bridging hydride and a total of 0.8% for the two phosphorus atoms.

With respect to electrocatalysis, we found that turnover of the system in the presence of a proton source (50 mM $HBF_4 \cdot Et_2O$, 5 equiv) in the MeCN electrolyte resulted in a ca. 9 s lag before disappearance of the FTIR bands of the parent complex **1**, fully consistent with electrocatalysis involving the generation of the 37-electron radical and fast protic attack to yield dihydrogen and restore the parent hydride cation **1**. Only after exhaustion of the acid was depletion of **1** in the thin layer observed.

Beyond their relevance to synthetic and natural di-iron catalysis, there is the wider aspect of the role of paramagnetic hydrides in other dihydrogen-evolving bioinorganic systems, including nickel−iron hydrogenase[1,27] and related model systems.[28] Nitrogenase concomitantly evolves dihydrogen with nitrogen fixation. Fe−μ-H−Fe intermediates have been proposed in the four-electron-reduced state of the FeMoco center of nitrogenase on the basis of EPR and electron−nuclear double resonance (ENDOR) measurements:[29] the $S = {}^1/_2$ signal is associated with A_{iso} = 23 MHz for the two symmetrically disposed ^{1}H atoms. This is the only other reported di-iron system where a unique bridging hydride has been characterized spectroscopically.[30]

In summary, paramagnetic metallohydrides are likely key intermediates in enzymic and molecular catalysis involving metallosulfur assemblies. Using an advanced FTIR spectroelectrochemical cell, DFT calculations, and EPR spectroscopy, we have now characterized the first discrete mixed-valence di-iron μ-hydride species. This is a valence-delocalized system, and isotopic-labeling studies have established that substantial radical character resides on the strongly coupled bridging hydride.

■ ASSOCIATED CONTENT

Supporting Information. Full experimental details, simulated EPR spectra, DFT coordinates, energy levels, and simulated IR spectra. This material is available free of charge via the Internet at http://pubs.acs.org.

■ AUTHOR INFORMATION

Corresponding Author
c.pickett@uea.ac.uk

■ ACKNOWLEDGMENT

This research was supported by the EPSRC and the University of East Anglia. The authors thank Dr. Fraser MacMillan for helpful discussions.

■ REFERENCES

(1) Tard, C.; Pickett, C. J. *Chem. Rev.* **2009**, *109*, 2245–2274.
(2) Gloaguen, F.; Rauchfuss, T. B. *Chem. Soc. Rev.* **2009**, *38*, 100–108.
(3) Zhao, X.; Georgakaki, I. P.; Miller, M. L.; Yarbrough, J. C.; Darensbourg, M. Y. *J. Am. Chem. Soc.* **2001**, *123*, 9710–9711.
(4) Dong, W.B.; Wang, M.; Liu, X. Y.; Jin, K.; Li, G. H.; Wang, F. J.; Sun, L. C. *Chem. Commun.* **2006**, 305–307.
(5) Morvan, D.; Capon, J. F.; Gloaguen, F.; Le Goff, A.; Marchivie, M.; Michaud, F.; Schollhammer, P.; Talarmin, J.; Yaouanc, J. J.; Pichon, R.; Kervarec, N. *Organometallics* **2007**, *26*, 2042–2052.
(6) van der Vlugt, J. I.; Rauchfuss, T. B.; Whaley, C. M.; Wilson, S. R. *J. Am. Chem. Soc.* **2005**, *127*, 16012–16013.
(7) Barton, B. E.; Rauchfuss, T. B. *Inorg. Chem.* **2008**, *47*, 2261–2263.
(8) Ezzaher, S.; Capon, J.-F.; Gloaguen, F.; Pétillon, F. Y.; Schollhammer, P.; Talarmin, J. *Inorg. Chem.* **2007**, *46*, 3426–3428.
(9) Barton, B. E.; Zampella, G.; Justice, A. K.; De Gioia, L.; Rauchfuss, T. B.; Wilson, S. R. *Dalton Trans.* **2010**, *39*, 3011–3019 .
(10) Zhao, X.; Georgakaki, I. P.; Miller, M. L.; Meija-Rodriguez, R.; Chiang, C.-Y.; Darensbourg, M. Y. *Inorg. Chem.* **2002**, *41*, 3917–3928.
(11) Jablonskytė, A.; Wright, J. A.; Pickett, C. J. *Dalton Trans.* **2010**, *39*, 3026–3034.
(12) Siegbahn, P. E. M.; Tye, J. W.; Hall, M. B. *Chem. Rev.* **2007**, *107*, 4414–4435.
(13) De Lacey, A. L.; Stadler, C.; Cavazza, C.; Hatchikian, E. C.; Fernandez, V. M. *J. Am. Chem. Soc.* **2000**, *122*, 11232–11233.
(14) Razavet, M.; Borg, S. J.; George, S. J.; Best, S. P.; Fairhurst, S. A.; Pickett, C. J. *Chem. Commun.* **2002**, 700–701.
(15) Chong, D.; Georgakaki, I. P.; Mejia-Rodriguez, R.; Sanabria-Chinchilla, J.; Soriaga, M. P.; Darensbourg, M. Y. *Dalton Trans.* **2003**, 4158–4163.
(16) Creco, C.; Bruschi, M.; De Gioia, L.; Ryde, U. *Inorg. Chem.* **2007**, *46*, 5911–5921.
(17) Zampella, G.; Greco, C.; Fantucci, P.; De Gioia, L. *Inorg. Chem.* **2006**, *45*, 4109–4118.
(18) Tschierlei, S.; Ott, S.; Lomoth, R. *Energy Environ. Sci.* **2011**, *4*, 2340–2352.
(19) Gloaguen, F.; Lawrence, J. D.; Rauchfuss, T. B.; Bérnard, M.; Rohmer, M.-M. *Inorg. Chem.* **2002**, *41*, 6573–6582.
(20) Best, S. P. *Coord. Chem. Rev.* **2005**, *249*, 1536–1554.
(21) For both **1** and **2**, the primary one-electron-reduced species decays to a second material. In MeCN, this second product has bands at 1943, 1899, and 1863 cm^{-1} and a broad feature at 1841 cm^{-1} for **1**, and that for **2** has bands at 1937, 1902, and 1870 cm^{-1}. In THF, the same bands are observed with better definition (see Figure 3, bottom).
(22) In earlier studies of the protonated systems, we showed by NMR spectroscopy that the only observable stable forms of **1** and **2** in solution are the transoid basal/basal isomers (see ref 11).

(23) The negative sign of A_{iso} was determined on the basis of the variation of the line width with m_I across the spectrum, with the largest negative m_I value being broadened least. For negative A_{iso}, the resonance at the lowest magnetic field is due to $m_I = -I$, while that at the highest magnetic field is due to $m_I = +I$. In Figure 4, the line at lowest magnetic field (highest g factor) is sharper than the line at highest field, indicating that A_{iso} is negative.

(24) $\gamma_D/\gamma_H = 0.153\,523$, where γ_D and γ_H are the magnetogyric ratios of ^2H and ^1H, respectively.

(25) The spin density in **1** is asymmetrical as a result of the propanedithiolate bridge, which flips rapidly on the EPR time scale.

(26) Wertz, J. E.; Bolton, J. R. *Electron Spin Resonance: Elementary Theory and Practical Applications*; McGraw-Hill: New York, 1972.

(27) Foerster, S.; van Gastel, M.; Brecht, M.; Lubitz, W. *J. Biol. Inorg. Chem.* **2005**, *10*, 51–62.

(28) Barton, B. E.; Rauchfuss, T. B. *J. Am. Chem. Soc.* **2010**, *132*, 14877–14885.

(29) Igarashi, R. Y.; Laryukhin, M.; Dos Santos, P. C.; Lee, H.-I.; Dean, D. R.; Seefeldt, L. C.; Hoffman, B. M. *J. Am. Chem. Soc.* **2005**, *127*, 6231–6241.

(30) Interestingly, Krusic and coworkers noted the generation of several paramagnetic hydride species upon irradiation of $Fe(CO)_5$ in the presence of H_2S. This included species assigned to two isomers of $Fe_2(CO)_6(\mu\text{-SH})_2(\mu\text{-H})$, for which an A_{iso} value of ~91 MHz was reported. See: Keizer, P. N.; Krusic, P. J.; Morton, J. R.; Preston, K. F. *J. Am. Chem. Soc.* **1991**, *113*, 5454–5456.